Journal of Biomechanical Science and Engineering

Vol. 3, No. 2, 2008

MR-Compatible Compression Device for In-Vitro Evaluation of Biomechanical Properties of Cartilage *

Vladimir JURAS**,***, Pavol SZOMOLANYI**,***,
Zuzana MAJDISOVA**,*** and Siegfried TRATTNIG**

**MR Centre - High Field MR, Department of Radiology, Medical University of Vienna, Vienna, Austria
***Institute of Measurement Science, Department of Imaging Methods, Slovak Academy of Sciences, Bratislava, Slovakia

Abstract

Objective: Purpose of the paper is to present and validate a device for cartilage compression for assessment of MR parameters (T1, T2, ADC) in cartilage explants before, during and after compression operating with novel features.

Design: This device fits into a BGA-12 micro-imaging gradient system capable of delivering 200mT/m. A 35 mm inner diameter resonator was used. The reproducibility and accuracy of cartilage compression possible with the device were evaluated. Sixteen human cartilage explants from knee joints were examined by delayed Gadolinium enhancement MRI of cartilage (dGEMRIC) for T1 mapping, T2 mapping and ADC measurements.

Results: Cartilage compression studies demonstrated both low inter-observer (CV 4.7 %) and intra-observer (CV 11.9 %) variation. No undesired movements were observed. The compressive piston could be moved with high accuracy (error ~ 1.07 %). The waterproof chamber of the compression device allowed contrast enhanced T1 mapping without repositioning the cartilage samples. Preliminary results of MR parameters depending on compression are presented.

Conclusions: In vitro MR cartilage compression studies are feasible with the custom-build device with high reproducibility and accuracy. Valuable information about biomechanical cartilage properties can be recorded using this device.

Key words: Cartilage, Compression, Relaxation Time, Diffusion, Compression Device

1. Introduction

Magnetic resonance imaging (MRI) is a very useful modality for cartilage imaging [1]. It is frequently used for noninvasive diagnosis of cartilage diseases, such as osteoarthritis [2-4], articular cartilage injury patients and for monitoring of conservative and surgical cartilage therapies [5-7]. However, early diagnosis of cartilage lesions using MRI still poses a problem since morphological alteration of cartilage tissue represents a relatively late manifestation which is preceded by biochemical and biomechanical changes in the cartilage. In addition, to the visualization of morphological structure of articular cartilage the visualization of changes in cartilage tissue (healthy and/or diseased) exposed to a static (or dynamic) load can provide important information regarding cartilage function. Investigators have used MRI to evaluate mechanical properties by measuring deformation in response to an applied load [8-10]. Some MR-compatible devices have been built to

*Received 15 Apr., 2008 (No. 08-0306)
[DOI: 10.1299/jbse.3.200]

provide controlled loading of cartilage explants and intact joints [11-13]. Recent in vivo studies demonstrated the ability to measure changes in cartilage volume with mechanical function (i.e., exercise) [14,15]. Other investigators have observed changes of T2 after load in-vitro [16-18] and in-vivo [19]. The common problem while comparing pre- and post-compression states is to align corresponding pixels (or regions of interest). To date, only a limited number of studies evaluating T1 and apparent diffusion coefficient (ADC) [20] in a post-compression state have been conducted. To our knowledge a contrast-enhanced study for dGEMRIC under compression has not been reported so far.

The purpose of our study was to introduce a specially designed compression device which can be used to reproducibly and accurately evaluate changes of MR parameters in cartilage explants under load. This device allowed us to keep samples in the solution and change the solution content "on the fly", a requirement to perform dGEMRIC. The feasibility of the device and compositional techniques to be applied within the device was evaluated, and, additionally the preliminary results of MRI parameters comparison between pre- and post-compression states are presented.

2. Materials and Methods

Experiments were performed on a Bruker 3T Medspec whole-body scanner (Bruker, Ettlingen, Germany). A BGA 12 micro-imaging gradient system capable of delivering a 200mT/m gradient, and 35 mm inner diameter resonator was used. The test equipment for micro-imaging of cartilage under compression consists of a micro-gradient (figure 3a), a coil holder (figure 3b) for fixing the coil, a custom built waterproof chamber for holding the sample (figure 3c), a further plastic chamber (figure 3f) and compression rod with a displacement scale (figure 3e). The micro-gradient system is actively shielded and water-cooled with an aperture diameter of 25 mm. In order to fasten the rig into the whole body 3T scanner two nylon screws fixed the rig to appropriate holes in the patient table.

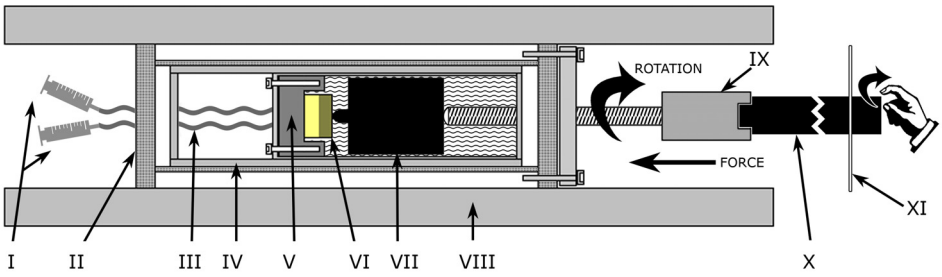

Fig. 1 Function diagram of compression device: I. Syringes used for liquid content swapping; II. Coil holder (fig 3.b); III. Hoses connected to waterproof chamber; IV. Coil with 35mm inner diameter; V. Plastic chamber; VI. Cartilage sample - brighter area represents bone tissue, darker area represents cartilage tissue; VII. Compressive piston - there are more types with different contact areas, the one depicted has contact area of 3mm^2; VIII. The body of the microgradient insert (fig. 3a); IX. Screw that produces compressive force with direction represented by the large left- arrow; X. 90 cm rod allows to perform compression out of the magnet; XI. Scale (fig. 3e) for exact displacement of compressive piston.

The feasibility of the compression device was determined by means of several parameters. First, the accuracy of compression rod rotation was evaluated. Movement of compression piston depends on screw pitch. 360º rotations were repeated twenty-one times after each imaging with standard protocol (details below). Each 360º rotation produces axial displacement of 1.50 mm.

Absence of compression device related movements was validated. Chamber filled with PBS solution only was imaged in the way that piston head and chamber body are visible on the images. Subsequently, distances between 1) piston axis and edge of image (left and right) and 2) chamber body and the edge of image (left and right) were acquired. We obtained 4 values (dL2, dL3, dR2 and dR3) as depicted on figure 1a. All values were measured in millimeters. After each acquisition compression was performed - in other words, piston head was displaced for 1.5 mm. This was repeated 7 times. Our aim was to validate that no undesired movements of any device parts appear after the compression process. Absolute standard deviation less than in-plane resolution (.234 mm in all measurements) was considered to be a sufficient confirmation of the device accuracy. Image reconstructions and distance measuring was performed with the help of ParaVision Software (Bruker, Ettlingen, Germany).

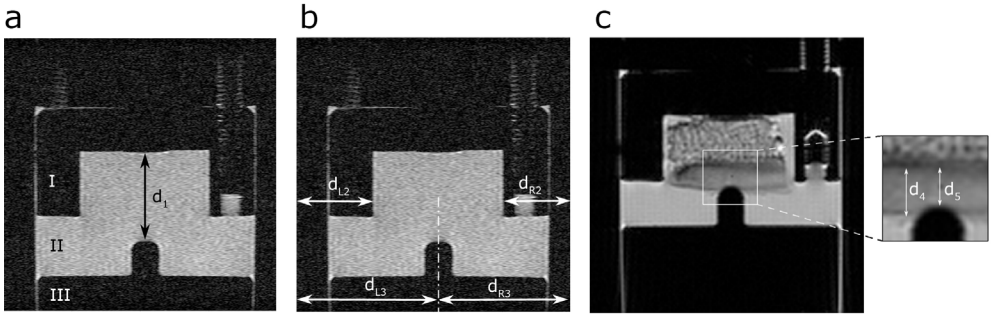

Fig. 2 MR images used for validating of stability of the compression device. a) measuring of the accuracy of the displacement of compression piston, d_1 is the measured distance between piston head surface and the bottom of the chamber (in millimeters); I - plastic chamber, II - PBS solution, III - compressive piston; b).d_2 and d_3 were used to show that no movements appear during the compression process; c) cartilage sample was used to prove accuracy of accomplishing 15% of cartilage thickness - observers were challenged to achieve expression (100 * d_5/d_4)% to be as close as possible to 15%.

Cartilage samples of human femoral condyle cartilage were obtained from 16 patients undergoing total knee joint replacement. At the time of surgery the cuts off were wrapped in gauze soaked in phosphate buffered saline (PBS) containing protease inhibitor and then frozen until required for testing. Subsequently, the specimens were thawed at room temperature and 10 x 10 mm blocks of cartilage-bone plugs were fashioned from the surgical femoral off cuts. These specimens were then inserted into the plastic specimen holder and inserted into the chamber which was filled with a solution of PBS with GdDTPA2- (Magnevist, Schering, Berlin, Germany) with a concentration of 1:500. Three independent observers performed compression of 15% of cartilage thickness. Each observer did it on the 6 different cartilage samples. Using data measured from three observers, we calculated the alpha coefficient and coefficient of variation for intra- and inter-observer variability of our measurements. An alpha coefficient value above 0.9 indicates excellent agreement among the measurements [21]. For statistical calculation SPSS statistical software (SPSS Inc, Chicago, IL) was used. For image acquisition a multi-slice multi-echo protocol was used with TR/TE 343 msec/15 msec. We acquired 10 slices of 1.5 mm thickness, with no intersection gap. Field of view was set to 30 x 30 mm. The imaging matrix was 128 x 96, reconstructed to 128 x 128 pixels images. Evaluation was performed on 512 x 512 pixels zoomed images.

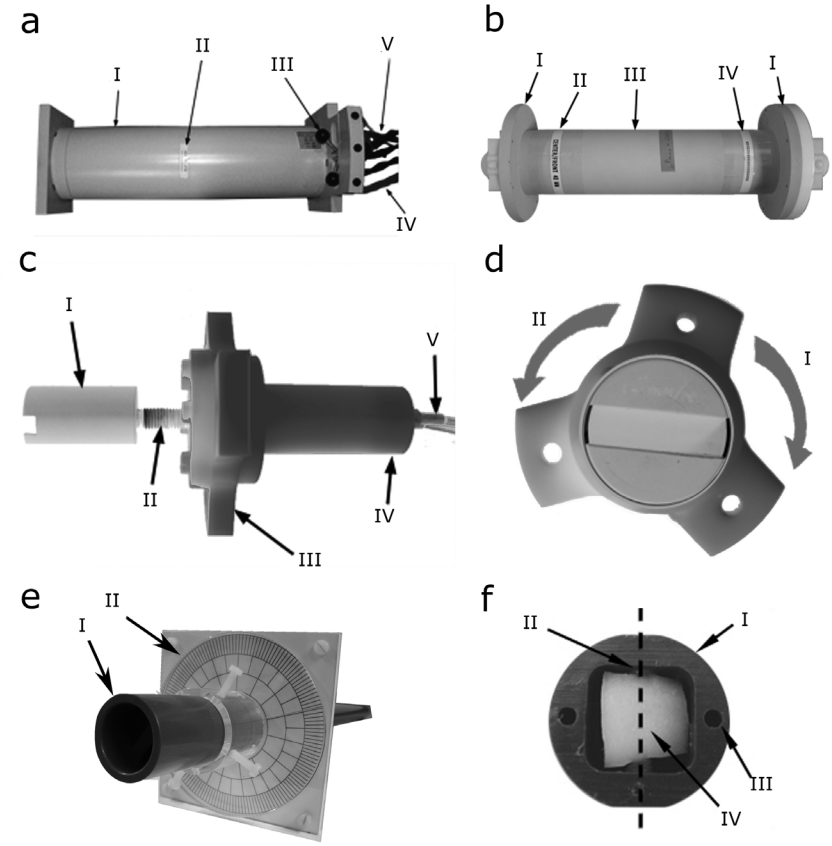

Fig 3. **a:** Micro-gradient system BGA 12: I – body of a device, II – center mark, III – top fixing screw, IV – hoses for water cooling, V – supply cables. **b:** Coil holder – top view: I – discs to fit this part into a micro-gradient insert, II – mark for correct direction, III – connecting cylinder, IV – mark for correct position in scanner. **c:** Sample holder – top view: I, II – screw for generating compression movement, III – milled disc for fixing holder to coil holder, IV – waterproof chamber with cartilage sample, V – slender hoses. **d:** Sample holder – left view: compression of cartilage is accomplished by rotating screw in direction I, decompression in direction II. **e:** I – compression rod, II – scale (the smallest segment corresponds to 1/150 mm). **f:** Sample holder: I – plastic body, II – screws for cartilage fixing, III – screw holes for holder fixing, IV – piece of the cartilage.

T1 mapping was realized by spin echo pulse sequence with inversion recovery, TI times were set to 15, 30, 60, 160, 400 and 2000 ms, for T2 mapping multi-echo multi-slice spin echo sequence with TE times 15, 30, 45, 60, 75 and 90 ms was used. ADCs were calculated from data from pulsed gradient spin echo (PGSE) with 6 different b-values (10.472, 220. 627, 452.8, 724.5 and 957.7). Each of parameters was calculated by fitting on pixel-by-pixel basis to appropriate function, T1 [22], T2 [22] and ADC [23]. Fitting routines were written in IDL (Interactive Data Language, Research Systems, Inc.) using mpcurvefit routine (Craig B. Markwardt, NASA/GSFC Code 662, Greenbelt, MD 20770; craigm@lheamail.gsfc.nasa.gov). Region of interests (ROI) were set in appropriate place where the intender was in contact with cartilage surface. Measurement setup and the specificity of the device allowed choosing one ROI only for pre- and post-compression state. Kruskall-Wallis ANOVA test was used to assess statistical significance of the difference in MRI parameters before and during compression.

3. Results

Accuracy of compression screw

Eighteen compression cycles were recorded with mean moving distance of 1.48 ± 0.03

mm. The mean difference from the expected distance (1.50 mm) was 1.07%. Measured values are summarized in the table 1.

#	d1	Δ	#	d1	Δ	#	d1	Δ
1	1.5	0.00	7	1.5	0.00	13	1.34	-0.16
2	1.43	-0.07	8	1.6	0.10	14	1.51	0.01
3	1.47	-0.03	9	1.47	-0.30	15	1.49	-0.01
4	1.7	0.20	10	1.41	-0.09	16	1.46	0.04
5	1.4	-0.10	11	1.55	0.05	17	1.5	0.00
6	1.41	-0.09	12	1.47	-0.03	18	1.5	0.00

Tab 1 Values that prove accuracy of compression piston displacement. Symbol # denotes measurement number, d1 denotes piston head displacement and Δ is difference from expected value (1.50 mm).

Stability of the compression device

The relative distance between chamber and edge of the image was 3.48 ± 0.05 mm for left side (dL2) and 2.22 ± 0.05 mm for right side (dR2). In percentage representation, standard deviation is approximately 1.3% and 2.4%, respectively. Measured distance between axis of piston head and the edge of the image was 8.43 ± 0.03 (0.36%) mm for left side (dL3) and 7.31 ± 0.02 (0.26%) for right side (dR3). Values are summarized in the table 2.

measurement #	d_{L2} [mm]	d_{R2} [mm]	d_{L3} [mm]	d_{R3} [mm]
1	3.4	2.17	8.44	7.32
2	3.46	2.17	8.44	7.27
3	3.52	2.29	8.44	7.32
4	3.52	2.23	8.44	7.32
5	3.52	2.29	8.44	7.32
6	3.46	2.17	8.44	7.32
7	3.46	2.23	8.36	7.32
Average [mm]	3.477	2.221	8.429	7.313
Std. Dev. [mm]	0.045	0.054	0.030	0.019
Std. Dev. [%]	1.304	2.430	0.359	0.258

Tab 2 Measured values according to fig. 2b.

	T1 [ms]	T2 [ms]	ADC [mm^2/s] × 10^3
pre-compression	173.13 (49.83)	27.70 (6.74)	1.04 (0.12)
post-compression	159.51 (42.08)	23.84 (6.08)	1.14 (0.11)
difference (in %)	-7.68	-13.93	8.74
p-value	0.232	<0.05	<0.05

Tab 3 Values of MRI parameters before and during compression. Values in brackets are standard deviations.

Inter- and intra-observer variability

Mean cartilage thickness was 2.75 ± 0.78 mm. The precision of compression piston displacement from the three independent observers showed good intra- (mean CV 11.9%) and inter-observer agreement (mean CV 4.7%). The alpha coefficient for intra-observer variability was good (0.872) and for and inter-observer variability was excellent (0.955).

Changes in T1, T2 and ADC during compression

Relaxation parameters T1 and T2 as well as ADC in pre- and post-compression states are shown in the Table 3. The results showed significant change in T2 (decrease) and ADC (increase). T1 decreased during compression, but the change was not statistically significant.

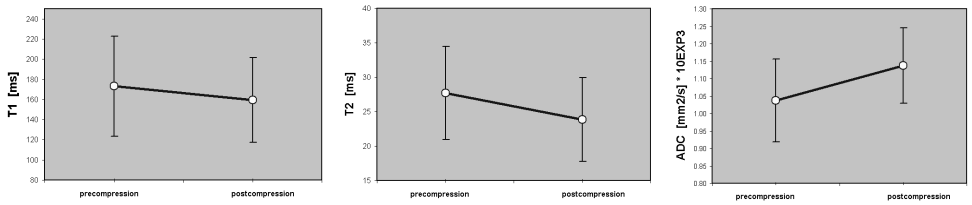

Fig. 4 Quantitative changes of MRI parameters while applied load

4. Conclusions

The main function of cartilage is to provide hydrostatic pressurization and evently distribute the load to the subchondral bone [24]. The unique ultra-structure of articular cartilage grants it a distinct ability to bear loads and to withstand stresses occurring in synovial joints. Mechanical properties of cartilage under compression have been studied widely [2,25,26]. Attempts have been made to develop an MR-compatible device to provide controlled loading of cartilage explants and intact joints [13,27]. Importantly, studies of cartilage under load are necessary to improve our understanding of the biochemical and biomechanical properties of articular cartilage. In particular, in vivo biochemical MR imaging continues to gains more importance by the use of dGEMRIC [28-30], T2 mapping [31], T1rho [32,33] mapping and diffusion-weighted imaging [34]. To validate these techniques under load in vitro compression studies are necessary.

In this study we reported a novel, custom built compression device for assessment of biomechanical properties of cartilage in vitro. One of the most important features of this device is its water-proof seal and the possibility to flush the specimen chamber in order to exchange the fluid, which allows dGEMRIC to be performed in vitro. Furthermore, multi-parametric MR of cartilage (dGEMRIC, T2, diffusion weighted imaging) can be performed without having to reposition the cartilage sample during examinations. The low standard deviations imply that the influence of movements of compression device and test rig during imaging is negligible. Furthermore, we have demonstrated that the compression piston can be moved accurately and reproducibly, since measured applied compression was 1.48 ± 0.03mm and differed from the expected value (1.5mm) by 1.07%. The inter- and intra-observer variability was 11.9% and 4.7%, respectively.

These results verified the accuracy and robustness of our compression device. No fluid leaks or movements of outer or inner parts were observed during the experiments.

During the course of the experiments we noted some minor short comings of the system; firstly, unwanted air bubbles were sometimes seen within specimen chamber, typically immediately after filling with liquid. Fortunately the air bubbles could be easily eliminated with repeated flushing of the liquid. All the measurements were performed at 12°C, which does not correspond to physiological temperature in vivo. This was necessary since the compression device is placed inside a micro-gradient system that must be cooled down. Thus, all parts of compression device are cooled down to temperature of cooling water. In the future, we plan to incorporate heating device in order to maintain the sample temperature as close to physiological body temperature as possible.

Preliminary results of the change of MRI parameters also proved the accuracy and robustness of the compression device. The significant decrease of T2 correlates to the collagen matrix deformation and is in the good agreement with previously published results, either ex-vivo [35] or in-vivo [17]. T1 is believed to be a marker of proteoglycans content. Although the total amount of proteoglycans content in the compressed area was not changed, the distribution of the proteoglycans over the volume was altered. Mean T1 decreased; however, the decrease was not statistically significant. The mean value of ADC increased of 8.74%. To the contrary, previously published results of the biochemical based studies showed the decrease of diffusivity in the cartilage after applied load [36]. Improving the evaluation procedures and increasing the number of samples should validate our results.

In conclusion, we have presented a novel compression device with unique properties including a watertight specimen chamber, the ability to exchange the bathing solution without moving any components; which is both accurate and reproducible. A particularly important application of the reported compression device is for the study of cartilage samples, including cartilage transplant samples, with different MR techniques with and without load in order to assess the biomechanical properties of different repair tissues compared to native cartilage.

Acknowledgement

We thank Reinhard Fuiko for providing cartilage samples.

Grant sponsors: Funding for this study was provided by Austrian Science Fund (FWF) FWF--Projekt P-18110-B15.

References

[1] Burstein D, Gray M. New MRI techniques for imaging cartilage. J Bone Joint Surg Am 2003;85-A Suppl 2:70-77.

[2] Eckstein F, Cicuttini F, Raynauld JP, Waterton JC, Peterfy C. Magnetic resonance imaging (MRI) of articular cartilage in knee osteoarthritis (OA): morphological assessment. Osteoarthr Cartilage 2006;14:A46-A75.

[3] Burstein D, Bashir A, Gray ML. MRI techniques in early stages of cartilage disease. Invest Radiol 2000;35(10):622-638.

[4] Recht MP, Goodwin DW, Winalski CS, White LM. MRI of articular cartilage: Revisiting current status and future directions. Am J Roentgenol 2005;185(4):899-914.

[5] Roberts S, McCall IW, Darby AJ, et al. Autologous chondrocyte implantation for cartilage repair: monitoring its success by magnetic resonance imaging and histology. Arthritis Res Ther 2003;5(1):R60-R73.

[6] Brown WE, Potter HG, Marx RG, Wickiewicz TL, Warren RF. Magnetic resonance imaging appearance of cartilage repair in the knee. Clin Orthop Relat R 2004(422):214-223.

[7] Trattnig S, Ba-Ssalamah A, Pinker K, Plank C, Vecsei V, Marlovits S. Matrix-based autologous chondrocyte implantation for cartilage repair: noninvasive monitoring by high-resolution magnetic resonance imaging. Magn Reson Imaging 2005;23(7):779-787.

[8] Hardy PA, Ridler AC, Chiarot CB, Plewes DB, Henkelman RM. Imaging articular cartilage under compression-cartilage elastography. Magnet Reson Med 2005;53(5):1065-1073.

[9] Neu CP, Hull ML, Walton JH. Heterogeneous three-dimensional strain fields during unconfined cyclic compression in bovine articular cartilage explants. J Orthopaed Res 2005;23(6):1390-1398.

[10] Neu CP, Hull ML, Walton JH, Buonocore MH. MRI-Based technique for

determining nonuniform deformations throughout the volume of articular cartilage explants. Magnet Reson Med 2005;53(2):321-328.

[11] Kaufman JH, Regatte RR, Bolinger L, Kneeland JB, Reddy R, Leigh JS. A novel approach to observing articular cartilage deformation in vitro via magnetic resonance imaging. J Magn Reson Imaging 1999;9(5):653-662.

[12] Herberhold C, Stammberger T, Faber S, et al. An MR-based technique for quantifying the deformation of articular cartilage during mechanical loading in an intact cadaver joint. Magnet Reson Med 1998;39(5):843-850.

[13] Herberhold C, Faber S, Stammberger T, et al. In situ measurement of articular cartilage deformation in intact femoropatellar joints under static loading. J Biomech 1999;32(12):1287-1295.

[14] Eckstein F, Lemberger B, Gratzke C, et al. In vivo cartilage deformation after different types of activity and its dependence on physical training status. Ann Rheum Dis 2005;64(2):291-295.

[15] Eckstein F, Tieschky M, Faber S, Englmeier KH, Reiser M. Functional analysis of articular cartilage deformation, recovery, and fluid flow following dynamic exercise in vivo. Anat Embryol 1999;200(4):419-424.

[16] Rubenstein JD, Kim JK, Henkelman RM. Effects of compression and recovery on bovine articular cartilage: Appearance on MR images. Radiology 1996;201(3):843-850.

[17] Liess C, Lusse S, Karger N, Heller M, Gluer CC. Detection of changes in cartilage water content using MRI T-2-mapping in vivo. Osteoarthr Cartilage 2002;10(12):907-913.

[18] Alhadlaq HA, Xia Y. The structural adaptations in compressed articular cartilage by microscopic MRI (mu MRI) T-2 anisotropy. Osteoarthr Cartilage 2004;12(11):887-894.

[19] Nag D, Liney GP, Gillespie P, Sherman KP. Quantification of T-2 relaxation changes in articular cartilage with in situ mechanical loading of the knee. J Magn Reson Imaging 2004;19(3):317-322.

[20] de Visser SK, Crawford RW, Pope JM. Structural adaptations in compressed articular cartilage measured by diffusion tensor imaging. Osteoarthritis Cartilage 2007.

[21] Cortina J. What is coefficient alpha? J Appl Psychol 1993;78:98-104.

[22] Rohrer M, Bauer H, Mintorovitch J, Requardt M, Weinmann HJ. Comparison of magnetic properties of MRI contrast media solutions at different magnetic field strengths. Invest Radiol 2005;40(11):715-724.

[23] Mlynarik V, Sulzbacher I, Bittsansky M, Fuiko R, Trattnig S. Investigation of apparent diffusion constant as an indicator of early degenerative disease in articular cartilage. J Magn Reson Imaging 2003;17(4):440-444.

[24] Grushko G, Schneiderman R, Maroudas A. Some Biochemical and Biophysical Parameters for the Study of the Pathogenesis of Osteo-Arthritis - a Comparison between the Processes of Aging and Degeneration in Human Hip Cartilage. Connect Tissue Res 1989;19(2-4):149-176.

[25] Eckstein F, Lemberger B, Stammberger T, Englmeier KH, Reiser M. Patellar cartilage deformation in vivo after static versus dynamic loading. J Biomech 2000;33(7):819-825.

[26] Kessler MA, Glaser C, Tittel S, Reiser M, Imhoff AB. Volume changes in the menisci and articular cartilage of runners - An in vivo investigation based on 3-D magnetic resonance imaging. Am J Sport Med 2006;34(5):832-836.

[27] Armstrong CG, Bahrani AS, Gardner DL. Invitro Measurement of Articular-Cartilage Deformations in the Intact Human Hip-Joint under Load. J Bone Joint Surg Am 1979;61(5):744-755.

[28] Bashir A, Gray ML, Burstein D. Gd-DTPA(2-) as a measure of cartilage degradation. Magnet Reson Med 1996;36(5):665-673.

[29] Allen RG, Burstein S, Gray ML. Monitoring glycosaminoglycan replenishment in cartilage explants with gadolinium-enhanced magnetic resonance imaging. J Orthopaed Res 1999;17(3):430-436.

[30] Regatte RR, Akella SV, Wheaton AJ, Borthakur A, Kneeland JB, Reddy R. T 1 rho-relaxation mapping of human femoral-tibial cartilage in vivo. J Magn Reson Imaging 2003;18(3):336-341.

[31] Mosher TJ, Dardzinski BJ. Cartilage MRI T2 relaxation time mapping: Overview and applications. Semin Musculoskel R 2004;8(4):355-368.

[32] Duvvuri U, Reddy R, Patel SD, Kaufman JH, Kneeland JB, Leigh JS. T-1 rho-relaxation in articular cartilage: Effects of enzymatic degradation. Magnet Reson Med 1997;38(6):863-867.

[33] Mlynarik V, Szomolanyi P, Toffanin R, Vittur F, Trattnig S. Transverse relaxation mechanisms in articular cartilage. J Magn Reson 2004;169(2):300-307.

[34] Miller KL, Hargreaves BA, Gold GE, Pauly JM. Steady-state diffusion-weighted imaging of in vivo knee cartilage. Magnet Reson Med 2004;51(2):394-398.

[35] Regatte RR, Kaufman JH, Noyszewski EA, Reddy R. Sodium and proton MR properties of cartilage during compression. J Magn Reson Imaging 1999;10(6):961-967.

[36] Quinn TM, Morel V, Meister JJ. Static compression of articular cartilage can reduce solute diffusivity and partitioning: implications for the chondrocyte biological response. J Biomech 2001;34(11):1463-1469.